AGU PUBLICATIONS

JGR

Journal of Geophysical Research: Earth Surface

RESEARCH ARTICLE
10.1002/2016JF004075

**Key Points:**
- Channel geometry trend breaks in the tidal-fluvial transition zone
- Trends in channel geometry differ from those in bed material grain size
- Channel properties in the Kapuashave a mixed character

**Supporting Information:**
- Supporting Information S1

**Correspondence to:**
K. Kästner,
karl.kastner@wur.nl

**Citation:**
Kästner, K., A. J. F. Hoitink, B. Vermeulen, T. J. Geertsema, and N. S. Ningsih (2017), Distributary channels in the fluvial to tidal transition zone, *J. Geophys. Res. Earth Surf.*, *122*, 696–710, doi:10.1002/2016JF004075.

Received 9 SEP 2016
Accepted 27 FEB 2017
Accepted article online 9 MAR 2017
Published online 28 MAR 2017



# Distributary channels in the fluvial to tidal transition zone

**K. Kästner[1], A. J. F. Hoitink[1], B. Vermeulen[2], T. J. Geertsema[1], and N. S. Ningsih[3]**

[1]Hydrology and Quantitative Water Management Group, Wageningen University and Research Centre, Wageningen, Netherlands, [2]Faculty of Engineering Technology, Water Engineering and Management, University of Twente, Enschede, Netherlands, [3]Research Group of Oceanography, Faculty of Earth Sciences and Technology, Bandung Institute of Technology, Bandung, Indonesia

**Abstract** Coastal lowland plains under mixed fluvial-tidal influence may form complex, composite channel networks, where distributaries blend the characteristics of mouth bar channels, avulsion channels, and tidal creeks. The Kapuas coastal plain exemplifies such a coastal plain, where several narrow distributaries branch off the Kapuas River at highly asymmetric bifurcations. A comprehensive geomorphological analysis shows that trends in the channel geometry of all Kapuas distributaries are similar. They consist of a short, converging reach near the sea and a nonconverging reach upstream. The two parts are separated by a clear break in scaling of geometrical properties. Such a break in scaling was previously established in the Mahakam Delta, which suggests that this may be a general characteristic in the fluvial to tidal transition zone. In contrast to the geometrical trend similarities, a clear difference in bed material between the main and side distributaries is found. In the main distributary, a continuous trend of downstream fining is established, similar to what is often found in lowland rivers. In the side distributaries, bed material coarsens in the downstream direction. This indicates an undersupply of sediment to the side distributaries, which may contribute to their long-term stability as established from historical maps. Tides may be the main agent preventing fine sediment to settle, promoting residual transport of fine material to the coastal ocean.

## 1. Introduction

River deltas are formed by deposition and reworking of sediment [*Davis Jr. and Dalrymple*, 2011]. Deltas take a characteristic appearance depending on the degree in which river discharge, wind waves, and tides contribute to sediment transport and morphological change [*Galloway*, 1975]. Across a single delta plain, the influence of river flow, wave action, and tides can vary, which locally affects the appearance of the delta. For example, the Mahakam forms a typical mixed river tide-dominated delta, with tidal channels often disconnected from fluvial distributaries (Figure 1). The tidal channels are highly sinuous and converge strongly, i.e., their cross-sectional area decreases exponentially in upstream direction, which is in contrast to most of the distributaries. *Sassi et al.* [2012] revealed a break in cross-section geometrical properties in the Mahakam distributaries, which separates tide-dominated reaches downstream from the river-dominated reaches further upstream. Here we report on a channel network which shows a similar break in scaling behavior and investigate the link with trends in grain size development. Our aim is to better understand downstream trends in channel geometrical properties and bed material grain size across the fluvial to tidal transition zone by focusing on the Kapuas lowland plain. The Kapuas forms a complex delta channel network (Figure 2). Individual distributaries blend the properties of mouth bar channels, avulsion channels, and tidal creeks. These three channel types are defined in greater detail hereafter.

Mouth bar channels are formed during delta progradation [*Olariu and Bhattacharya*, 2006] as a consequence of continuous deposition of sediment in front of distributary outlets. These mouth bar deposits develop into islands over time, after which two new channels bifurcate around them [*Mikhailov*, 1966; *Edmonds and Slingerland*, 2007]. If undisturbed by waves and tides, distributary channels recursively bifurcate around mouth bars during progradation, forming a delta with channels radiating from a single delta apex [*Andren*, 1994; *Mikhailov*, 1970]. The resulting distributary channel network features a fractal appearance [*Marciano et al.*, 2005]. Due to deposition at the mouth, the distributaries are wide and shallow, and due to decreasing discharge with increasing bifurcation order, width and depth decrease in the downstream direction. Mouth bar

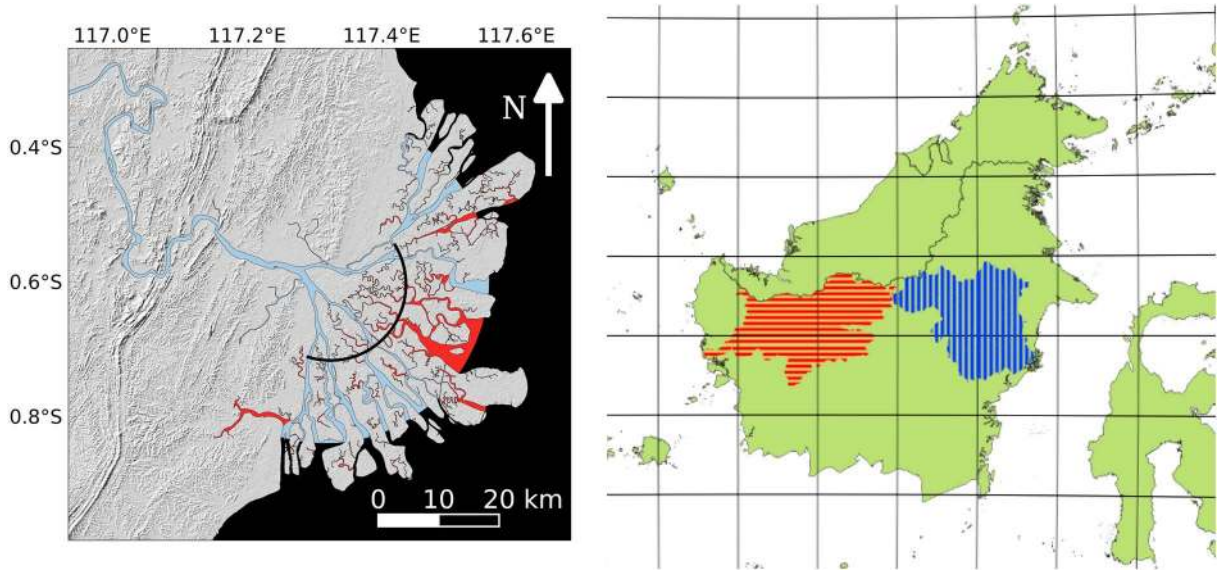


**Figure 1.** (left) Distributaries (blue) and tidal channels (red) in the Mahakam Delta. Gray shading indicates relief from SRTM data. The semicircle corresponds to the distance from the delta apex where the channel geometry changes from fluvial to tidal form (adapted from *Sassi et al.* [2012]). (right) Location of the Kapuas (red horizontally hatched) and Mahakam (blue vertically hatched) catchments on the island of Borneo.

formation requires sufficient inflow and sediment supply from the river [*Edmonds and Slingerland*, 2007]. The Wax Lake delta is a typical example of a delta composed of mouth bar channels [*Roberts et al.*, 1980]. Interaction between the radial spreading of the flows from neighboring distributary channels can form bathymetric depressions termed interdistributary troughs, which can complicate the channel pattern [*Shaw et al.*, 2016].

Distributary channels can also be created by avulsion, when, mostly during large flood events, the river bifurcates and takes a new course along a path with slope advantage [*Slingerland and Smith*, 1998; *Stouthamer et al.*, 2011]. Once a new avulsion channel is established, the old distributary may slowly be abandoned. This process can lead to cyclic delta complex switching, which occurs, for example, in the Mississippi [*Coleman*, 1988]. If avulsions occur more frequently than channels are abandoned, an anastamosing pattern with multiple channels running along the alluvial plain develops, extending the delta far upstream of the mouth bar complex [*Makaske*, 2001]. Albeit part of the delta architecture where waves and tides prevail, these distributaries often remain of fluvial nature. There is net sediment throughput in stable conditions, and their width-to-depth ratio is similar to that of single thread rivers. Anastamosing channel patterns can be found in many deltas around the world, for example, in the Parana [*Stevaux and Souza*, 2004], the Mackenzie [*Emmerton et al.*, 2007], the Pearl [*Wang et al.*, 2004], and the Lena [*Costard and Gautier*, 2007].

Tidal creeks can grow by headward erosion on tidal flats. They can be sole conveyors of tides and local runoff and do not need to receive river inflow [*D'Alpaos et al.*, 2005]. Tidal channels often form dentritic networks, where channels recursively branch off in the upstream direction at bifurcations with right angles [*Dalrymple et al.*, 2012]. These channels often interconnect to form islands [*Fagherazzi*, 2008]. The inlet size of a tidal channel is related to the tidal prism [*Jarrett*, 1976; *D'Alpaos et al.*, 2009], and width strongly converges with the reduction of the tidal prism in the upstream direction [*Pillsbury*, 1940; *Myrick and Leopold*, 1963; *Wright et al.*, 1973; *Fagherazzi and Furbish*, 2001; *Davies and Woodroffe*, 2010]. Typically, tidal channels are strongly meandering; their curvature decreases toward the channel outlet. The shape of the meander loops is more symmetric than that of fluvial meanders, due to the bidirectional flow [*Marani et al.*, 2002]. If there is no inflow from upstream, then there is no net sediment transport in stable tidal channels, similar to equilibrium estuaries [*Seminara et al.*, 2012]. The width-to-depth ratio of tidal channels is lower than that of mouth bar distributaries [*Marani et al.*, 2002]. Contrary to mouth bar distributaries, the depth of tidal channels increases in downstream direction with increasing gross discharge, although the depth convergence is smaller than the width convergence [*Savenije et al.*, 2008]. The Sundarbans represent one of the most extensive tidal creek systems worldwide, located in the Ganges-Brahmaputra Delta [*Passalacqua et al.*, 2013].

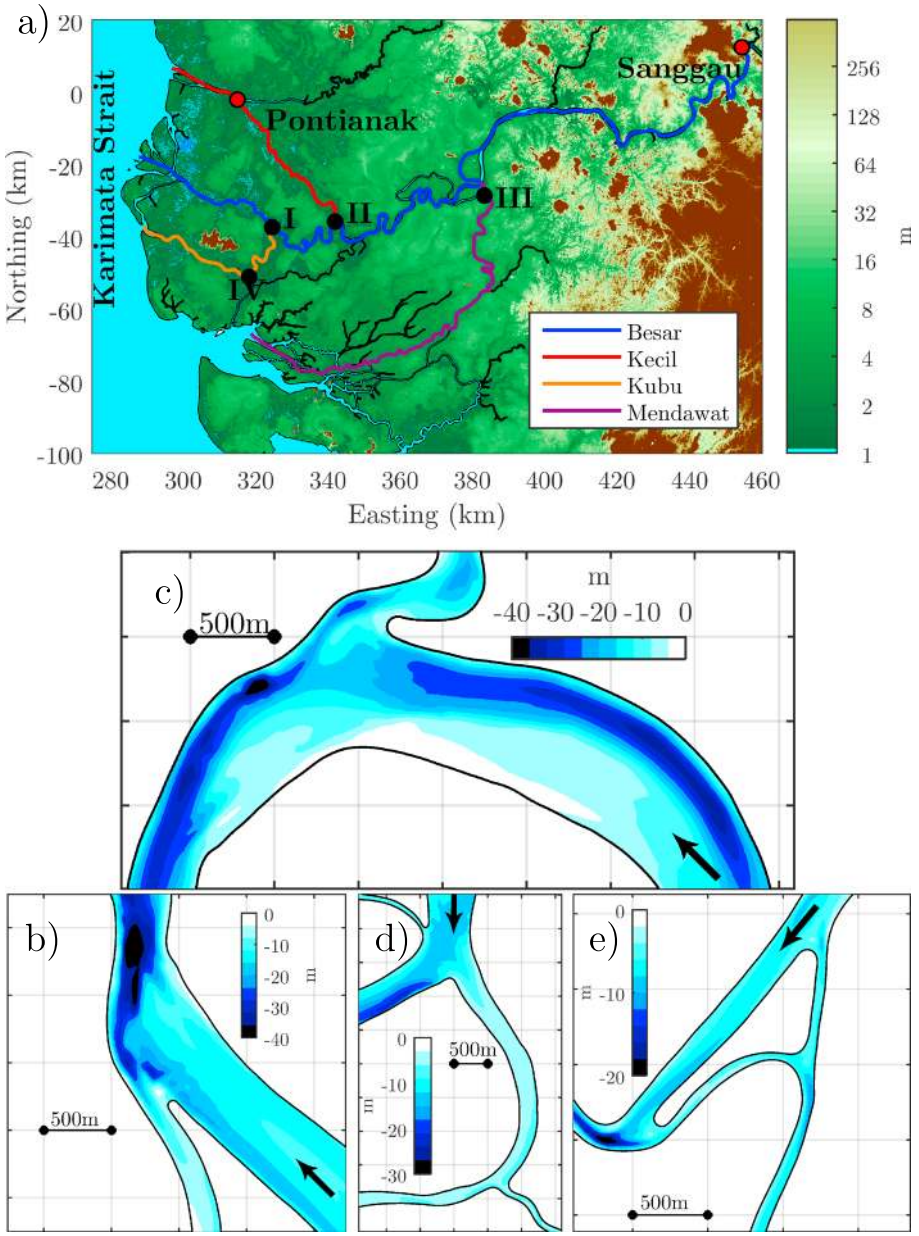


**Figure 2.** Topography of the Kapuas coastal plain with elevation from SRTM data (a); bathymetry of bifurcations: Kapuas Besar-Kubu (b), Kapuas Besar-Kapuas Kecil (c), Kapuas Besar-Mendawat (d), and South Kubu (e; neck cutoff due to dredging).

The along-channel trends of discharge differ between mouth bar channels, tidal creeks, and avulsion channels. As the discharge changes, the cross-section geometry adapts accordingly. The concept of downstream hydraulic geometry can be used for channel comparison. In hydraulic geometry, the relations between hydraulic parameters such as width and depth on discharge are expressed as power laws. In general, width and depth increase with increasing discharge [*Leopold and T. Maddock Jr*, 1953]. A recent review was compiled by *Eaton* [2013]. Similar to the channel geometry, the bed material grain size often has a distinct along-channel trend, which can be used to identify the morphological setting. Grain size of river sediment typically decreases in the downstream direction, due to abrasion and selective transport [*Snow and Slingerland*, 1987; *Hack*, 1957; *Frings*, 2008]. As the transport of sediment depends on the grain size, it influences the planform of fluvial channels [*Schumm*, 1985] and affects the morphology of deltas [*Orton and Reading*, 1993; *Geleynse et al.*, 2011]. Empirical hydraulic relationships including grain size have been proposed for fluvial channels

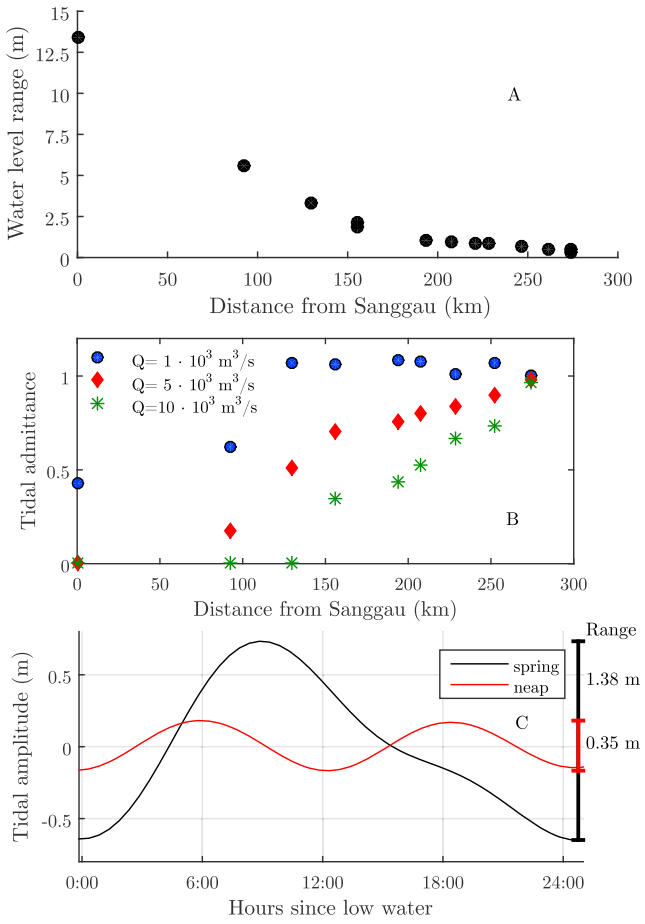


**Figure 3.** (a) Water level range, (b) admittance of the tidal wave along the Kapuas River, and (c) predicted spring (black) and neap (red) tide at the Kapuas River mouth [*Egbert and Erofeeva*, 2002].

[*Wilkerson and Parker*, 2010], yet little is known about the grain size trends in the fluvial to tidal transition zone, where bidirectional flow may cause a local maximum of grain size in estuaries [*Dalrymple and Choi*, 2007].

### 1.1. Field Site

The Kapuas is the largest river on the island of Borneo with a catchment size of $9.9 \cdot 10^4$ km$^2$. It is draining into the shallow Karimata strait, which separates Borneo from mainland Asia and the island Sumatra. The discharge is subject to strong seasonal variation associated with the monsoon [*Hidayat et al.*, 2016]. The Kapuas River is the main waterway in West Kalimantan, serving inland transportation. With the harbor of Pontianak at its mouth, it connects the province to the archipelago. The city of Pontianak relies on the river as a source of fresh water and fish but is subject to salinity intrusion and flooding during seasonal extremes. The Kapuas River is not yet controlled by man-made structures. Human influence is mostly indirect such as by development of palm oil plantations, which quickens rainfall runoff and increases sediment supply [*Buschman et al.*, 2012]. Despite the widespread development of oil palm plantations, the Kapuas River system can still be considered a relatively pristine setting.

Between 2013 and 2015, the Kapuas River was surveyed from the sea to the city of Sanggau, located 300 km upstream. Throughout this paper, distances are given along the river with respect to Sanggau. Where appropriate, the corresponding distances to the sea are provided in parentheses, e.g., Sanggau 0 km (300 km). For the first 100 km downstream of Sanggau, the Kapuas flows through a valley before entering the alluvial plain. Along the alluvial plain, several small distributaries branch off and the river forms a complex channel network (Figure 2), although most discharge reaches the sea through the main distributary: the Kapuas Besar. The bifurcations are highly asymmetric, such that the flow entering the side channel curves around a spit (Figures 2a–2d). The main distributary terminates in a delta fan with 15 km radius. The delta fan has one large trifurcation just downstream of the apex and five outlets. The three small distributaries are named Mendawat,

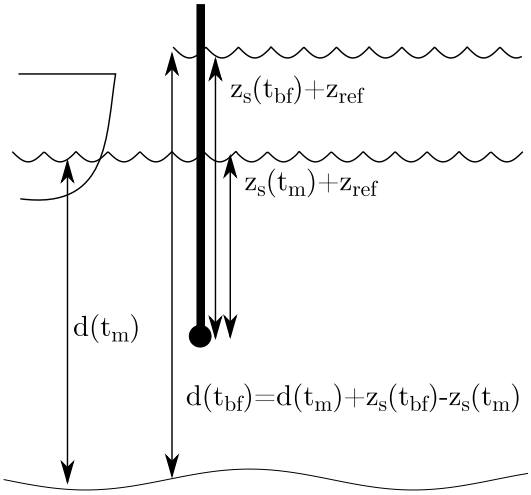


**Figure 4.** Determination of the bankfull depth from the depth sounded at an arbitrary water level. The depth at times of bankfull flow $d(t_{bf})$ is increased by the difference of the water level at times of bank full flow $z_s(t_{bf})$ and the water level at the time of measurement $z_s(t_m)$. The altitude $z_{ref}$ of the water level gauge with respect to the geodetic datum does not need to be known.

Kapuas Kecil, and Kubu. They branch off at 130 (159), 203 (87), and 241 (49) km, as indicated in Figure 2. The Kapuas Besar is meandering and has no major confluences downstream of Sanggau. The Mendawat and Kubu flow toward the south and are connected to a network of tidal creeks. The small distributaries show a meander pattern similar to the Kapuas Besar, and receive a disproportionately large inflow, with respect to their size.

During the monitoring period from October 2013 to May 2015 the daily averaged discharge ranged between 900 $m^3\ s^{-1}$ and 9500 $m^3\ s^{-1}$ at Sanggau. The water level range exceeds 9 m at Sanggau and gradually decreases in downstream direction to 2 m at 150 km. At this point, the downstream curve of the water level range has a pronounced break (Figure 3a). Averaged over a Metonic cycle, the tidal range in the Karimata Strait at the Kapuas River mouth is 1.35 m at spring tide and 0.35 m at neap tide (Figure 3b). The tidal form factor is 2.5, based on which the tides can be classified as mixed, mainly diurnal [*Pugh*, 1987]. Propagation of tides in the river strongly depends on discharge [cf. *Hoitink and Jay*, 2016]. Similarly to the water level range, the tidal amplitude development has a pronounced drop at the transition between the alluvial plain and the upstream valley. At low flow, the tide propagates until 130 (160) km without being considerably attenuated. From there on a gradual attenuation sets in (Figure 3c), so that the tidal amplitude in Sanggau is still 40% of the tidal amplitude at sea. At normal flow, the tide is also attenuated along the alluvial plain, but the attenuation is stronger beyond 130 km so that it does not reach Sanggau. At high flow, tides are gradually damped from the sea and fade out at 130 km.

## 2. Methods

### 2.1. Field Data Collection

Our survey of the Kapuas River reached from the sea until Sanggau, including the Kapuas Besar, Mendawat, Kapuas Kecil, and Kubu distributaries. The survey lasted from October 2013 to April 2015. Flow conditions ranged from base flow to bankfull flow during this period. The bathymetry was surveyed with a single beam echo sounder. We measured the bathymetry one time by crossing the river at an interval of one river width and a second time by following the river along its center [*Vermeulen et al.*, 2014]. Only a basic GPS with low vertical accuracy was available during the initial survey. An additional survey with a carrier phase and TerraStar-corrected GPS took place in November 2016. This survey consisted only of two along-river tracks. The two tracks followed the left and right river banks, respectively, with an approximate distance to the river bank of one fourth of the cross-section width. We determined the bankfull depth by combining the sounded bathymetry with surface level measurements recorded at 15 stations across the study area. Bed material was sampled with a Van Veen grabber. Three samples across the river were collected every 2.5 km, in total 411 samples. In the fan-shaped delta, bed material was sampled only in the central channel. At a few locations of interest, the sampling density was increased, and at several other locations no samples could be retrieved, presumably due to the presence of compact clay, gravel, or wooden debris. Samples were dried and sieved into separate size classes. For each sample, 200 g dry material was processed. Cohesive samples were crushed before sieving. American Society for Testing and Materials E11 sieves were used with a mesh size ranging between 0.045 and 4.75 mm, spaced by a factor of 1.4 [*American Society for Testing and Materials E11-16*, 2016].

### 2.2. Data Analysis

Channel width and curvature were extracted from Landsat images (Courtesy of the U.S. Geological Survey. Data available at https://earthexplorer.usgs.gov). At first, pixels were classified either as land or water, and then the bank line was extracted at the interface. Sounded depth was transformed to bankfull water level with

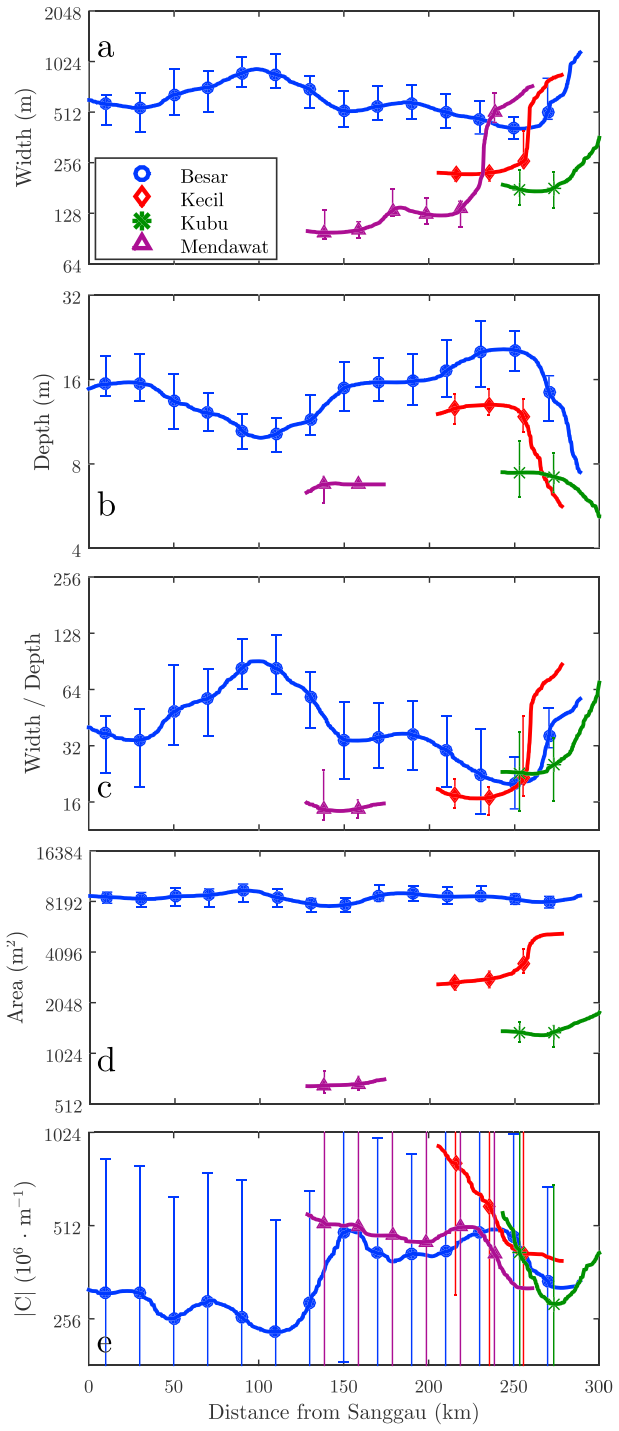


**Figure 5.** Downstream channel geometry of the Kapuas River; the lines indicate the median, and candlesticks indicate the 16th and 84th percentiles within the filter range. (a) Channel width, (b) bankfull depth, (c) width-to-depth ratio, (d) cross-sectional area, and (e) channel curvature.

the instantaneous water level (Figure 4). We employ the model by *Kukulka and Jay* [2003a, 2003b] to infer the instantaneous water level from the stage measured at Sanggau and tide predicted in the Karimata strait and use the data collected at the gauging stations for model calibration. Bankfull water level was defined as the water level averaged over a lunar day occurring during high flow ($10^4$ m$^3$ s$^{-1}$). Error in the conventional GPS altitude with respect to the bed elevation change along the surveyed reach inhibited accurate vertical referencing of the bed elevation. The echo sounder data were resampled to a 10 m resolution and then interpolated to a mesh. The cross-sectional area was determined at a 50 m interval by integrating the depth across the section. Channel depth is here defined as the ratio of area and top width. Due to the absence of extensive mudflats and flood plains, the channel widths are fairly constant in the studied area.

We analyzed the field data in two ways: first, by spatially filtering the parameters of channel geometry and grain size. Regarding the channel geometry, width ($W$), bankfull depth ($D$), aspect ratio ($W/D$), cross-sectional area ($W \cdot D$), and curvature ($C$) were analyzed. Those parameters of channel geometry were sampled at a 50 m interval and then spatially filtered with a weighted quantile filter. A Hanning window of 20 km length was used as a filter window. Within the filter range, the weighed median as well as the 16th and 84th quantiles were determined. A quantile filter was used as it is robust to outliers and preserves breaks [*Arce et al.*, 1998]. We explain the filter algorithm in detail in the supporting information. Regarding channel curvature, the filter was applied to the absolute value. Parameters of hydraulic geometry were plotted on logarithmic scale to the basis two. The bed level with respect to the WGS 84 was determined from the additional bathymetry data collected in 2016. The along-river tracks of this measurement were filtered with a weighed median filter and a Hanning window of 20km length to remove perturbations by bed forms and scour holes.

For each sample, the median ($D_{50}$), 16th ($D_{16}$), and 84th ($D_{84}$) percentiles as well as the standard deviation and skewness of the grain size distribution were computed on log scale. Standard deviation and skewness are given as nondimensional grain size $\log_2(D/1\ \text{mm})$ and for clarity denoted as $\phi$. Grain size itself is for better readability retransformed to millimeters. As for the channel geometry parameters, the grain size parameters

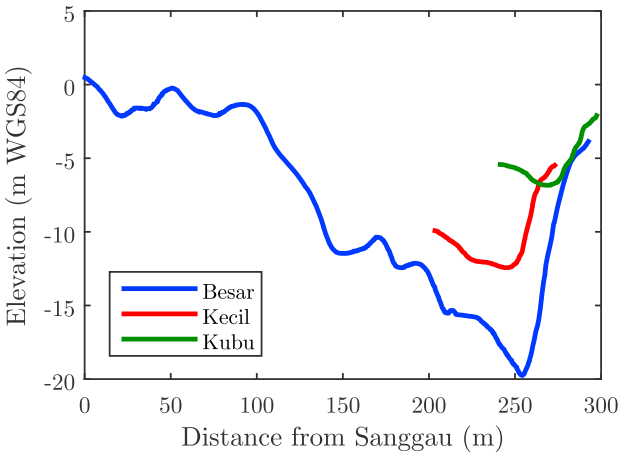


**Figure 6.** Bed level of the Kapuas River, candlesticks indicate 16th and 84th percentiles within the filter range of 20km; detailed bathymetric maps of the bifurcations are provided in Figure 2.

were spatially filtered with a weighed quantile filter. In addition, the histograms of the grain size distribution were averaged for each reach and plotted side by side. For each histogram bin, the trend along the reach was estimated as the difference of the average histogram in the upstream and downstream half of the reach. This allows to interpret grain size trends in terms of sediment transport and deposition, applying theory of selective transport [*McLaren*, 1981]. As small grains are transported at a higher rate than larger grains, the grain size distribution changes along the direction of transport. *McLaren* [1981] developed this concept to determine the direction and regime of sediment transport. If the grain size distribution at the source is uniform, the sediment becomes finer, better sorted, and more skewed in the downstream direction. As the grain size distribution in the Kapuas are far from uniform, the trends of statistical parameters of the grain size distribution are more complex. There the transport regime is directly derived from the histograms (Figure 8) rather than from the statistical moments (Figure 7). In addition the parameter distribution for each reach, i.e., the distribution of the mean, standard deviation, and skewness of the bed material samples, was then estimated with kernel density functions [*Scott*, 2015]. As a convolution Kernel, a Hanning-window of $1\phi$ width for the median grain size and $1/2\phi$ for the standard deviation were chosen.

## 3. Results

### 3.1. Channel Geometry

In the main distributary, three reaches with distinct trends of channel geometry can be distinguished. These correspond to the upstream valley, the alluvial plain, and the delta fan. In the upstream valley, channel width increases from 590 m at Sanggau to 910 m at the upstream limit of the alluvial plain, which corresponds to 100 (190) km (Figure 5a). Bankfull depth decreases in the latter reach from 15 m to 10 m (Figure 5b). There is a strong increase of the width-to-depth ratio from 40 to 90 (Figure 5c) but only a slight increase of the cross-sectional area from 8793 to 9500 $m^2$ (Figure 5d). The transition from the valley to the alluvial plain is also distinguished by an increase of curvature (Figure 5e). Along the alluvial plain, the Kapuas gradually narrows and reaches a minimum width of 400 m at 255 km (35 km), not far upstream from the delta apex. Parallel to the decrease in width, the bed level drops (Figure 6) so that the depth reaches a maximum of 20 m at the same place where the width obtains its minimum. Between the bifurcation with the Kapuas Kecil and the delta apex the Kapuas Besar has several deep scour holes with depths up to 55 m. The width-to-depth ratio decreases to 20 along the alluvial plain, due to the opposite trends in width and depth. For the same reason, the cross-sectional area remains nearly constant along the alluvial plain. The curvature first increases in the upstream part of the alluvial plain and remains high until 240 km, from where it reduces gradually toward the sea. From 255 km (35 km) downward, the Kapuas Besar gradually widens before splitting into the five branches. Summed over the branches, the total width continues to increase along the delta. The depth decreases throughout this last reach. All delta branches terminate in shallow mouth bars, where the bed almost emerges at low tide. As the width increases faster than depth decreases, the cross-sectional area increases toward the sea throughout the delta. However, the area increase is relatively small.

The side distributaries are considerably narrower and shallower than the Kapuas Besar. The Kapuas Kecil is the largest, and the Mendawat is the smallest of the side distributaries. Water level ranges over more than 3 m at the most upstream bifurcation, where the Mendawat branches off the Kapuas Besar. At this bifurcation, depth and area ratios are more extreme during low flow conditions than those at bankfull flow. The two downstream bifurcations have a particular shape, where the flow curves around a spit before entering the small distributary; see insets in Figure 2. The upstream bifurcation is a double bifurcation, where the Mendawat

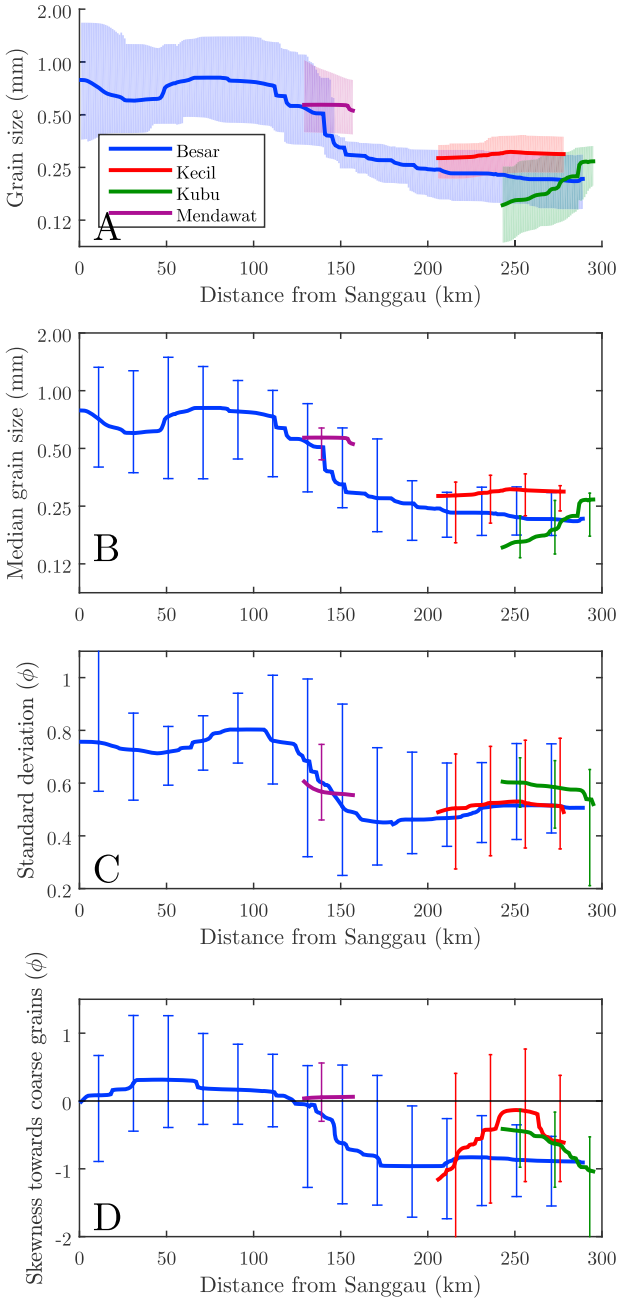


**Figure 7.** Median $D_{50}$ (a and b), standard deviation (c) and skewness (d) of the bed material grain size distribution along the Kapuas River. Shaded area in Figure 7a indicates range between $D_{16}$ and $D_{84}$ of the grain size distribution; (Figures 7a–7c) candlesticks indicate the 16th and 84th quantile of the respective parameter within the filter range.

branches off a local avulsion channel, running around an island. Similar to the Kapuas Besar, the upstream parts of the side channels consist each of a fluvial reach with constant cross section and of a funnel-shaped tidal reach that widens toward the sea. The transition is clearly visible as breaks in the downstream trend of width and depth (Figures 5a and 5b). Upstream of the break, the width-to-depth ratio remains constant along the channel. The transition to the funnel-shaped section in the Kapuas Kecil coincides with the Landak confluence at 255 km (22 km), where the cross-sectional area increases abruptly by 73%. The distance between the bifurcation toward the sea is 12 km shorter through the Kapuas Kecil than through the Kapuas Besar. The Mendawat is met at a confluence at 171 km, bifurcates at 191 km, and further down merges into a tidal creek system. Only the upstream part of the Mendawat was surveyed. Similar to the Kapuas Besar, the surveyed outlets of the Kapuas Kecil and Kubu feature shallow bars before debouching into the Karimata Strait. For reasons of shipping toward the harbor of Pontianak, the mouth of the Kapuas Kecil is regularly deepened by dredging, making it less shallow that of the other distributaries, but this does not remove the overall trend. Depth decreases throughout the funnel-shaped reach from 15 m to 5 m. The curvature development in the Mendawat channel is similar to that of the Kapuas Besar. It remains constant in the upstream reach before decreasing toward the sea. The curvature values in the Kapuas Kecil and Kubu are higher than in the Kapuas Besar. Both in the Kapuas Kecil and in the Kubu, curvature decreases toward the sea not far downstream of the bifurcation. There is no break in the downstream trend of curvature.

### 3.2. Bed Material Grain Size Distribution

Bed material in the Kapuas between Sanggau and the sea consists of coarse to fine sands. Material in sharp outer bends consists of compact clay, with an increasing amount of gravel throughout the upstream valley. At most of these locations, no material could be sampled with the Van Veen grabber. In total, less than 5% of all samples were void or composed of either gravel or compact clay. These locations were excluded from the analysis. Although some gravel and bed rock is present in the valley, the bed material consists predominantly of sand, and the gravel-sand transition is located further upstream than Sanggau. From Sanggau to 110 km (180 km) the bed material consists of coarse sand, with a median grain size of 0.7 mm (Figures 7a and 7b). The standard deviation is 0.77$\phi$, and the distribution is skewed toward

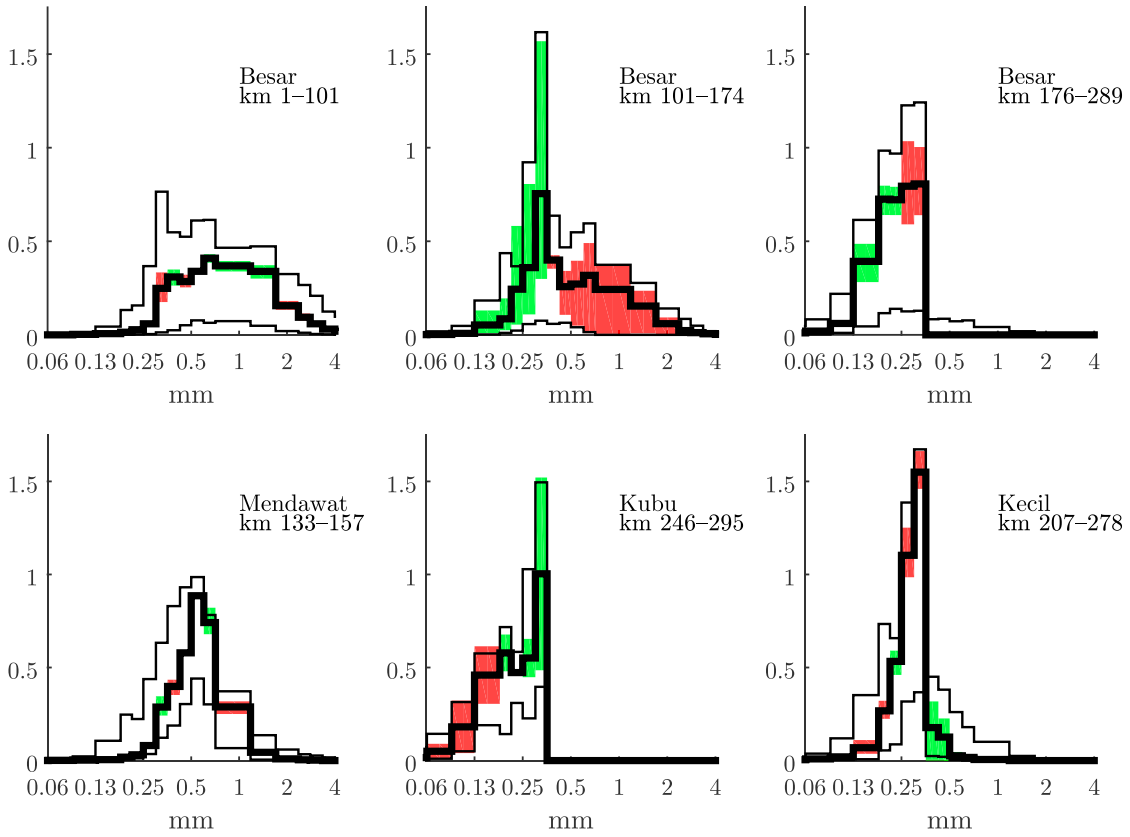


**Figure 8.** Histograms of the grain size distribution by reach; bars indicate the 16th, 50th, and 84th percentiles of each bin; and green areas indicate gains and red area indicate loss in downstream direction.

coarser grains (Figures 7c and 7d). In this reach, there is no considerable downstream trend of the median grain diameter, standard deviation, or skewness (Figure 7). At the foot of the alluvial valley, rapid fining sets in. Between 110 and 150 km grains larger than 0.35 mm are removed from the grain size distribution. In this reach, along-channel changes of the grain size distribution are much larger than in the reaches further upstream and downstream (Figure 8). The removal of coarse material causes an even more rapid decrease of the standard deviation and makes the grain size distribution skewed toward finer grains. Downstream of 150 km, the material consists of medium and fine sand. The median grain size decreases from 0.30 mm to 0.22 mm at the river mouth. The largest size fraction remains close to 0.35 mm, the $D_{84}$ decreases only marginally from 0.35 mm to 0.30 mm, while the $D_{16}$ decreases from 0.26 mm to 0.14 mm. Downstream fining continues throughout the delta fan. Upstream of the mouth bar, the grain size increases slightly. The standard deviation between 150 km and the outlet is 0.48$\phi$ and slightly increases toward the sea. The grain size distributions are skewed toward finer grains. Downstream of 240 km, coarse sediment was found on top of finer sediment, and an increasing number of samples concreted during drying, although only a few samples contained fractions smaller than 65 μm. The amount of silt could be slightly underestimated, as it is known that dry sieving is not suitable for analysis of silt samples [*Xiaoqing and Yang*, 2003]. The standard deviation of the grain size distribution does not continuously decrease in the downstream direction. This can also be seen in the bivariate plot of median grain size and standard deviation (Figure 9b). Samples of intermediate size are better sorted than samples consisting of fines and large material. The standard deviation decreases with the median grain size, up to 0.35 mm, but increases again for decreasing median grain sizes below 0.35 mm. The local variation of the grain size within the range of the filter window is large compared to the change due to downstream fining. Coarse and fine samples were often found within the same cross section. Between 150 km and the mouth, the 16th and 84th percentiles of the median grain size of individual samples are 0.35 mm and 0.18 mm, respectively (Figures 7b and 9e). Along-channel trends explain only half of the variance between samples ($R^2 = 0.52$).

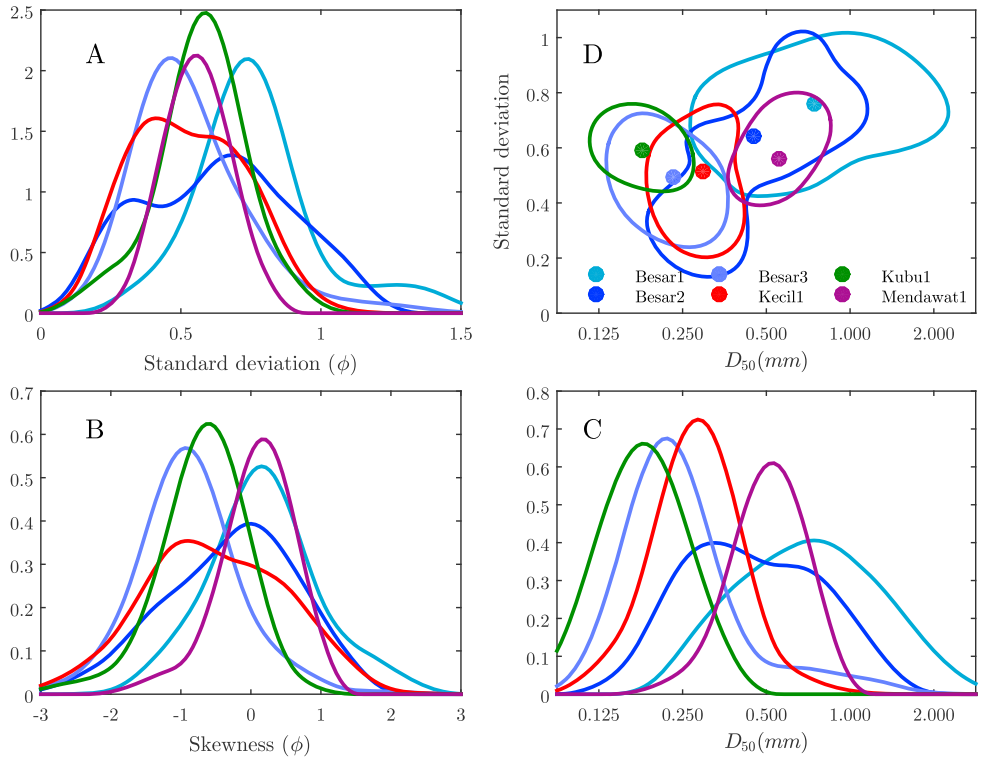


**Figure 9.** Distribution of the (a) median, (b) standard deviation, and (c) skewness among the samples grouped by reach as well as (d) joint distribution of median and standard distribution. The contour lines contain 68% of the samples of each reach.

Consistent with downstream fining in the main distributary, the initial grain sizes in the side distributaries directly after branching off are lower when the bifurcation is located further downstream. Thus, the grain size is coarsest in the Mendawat and finest in the Kubu. At the bifurcations, there is only a small difference between grain sizes in the side distributaries and in the main channel. The median grain size in the Kapuas Kecil is slightly coarser, and bed material in the Kubu channel is slightly finer than that of the Kapuas Besar (Figure 7a). The most striking downstream trend difference between the side distributaries and the main distributary is seen in the development of grain sizes. The material in the Kapuas Kecil and Kubu distributaries coarsens in downstream direction. The trend of coarsening is stronger in the Kubu distributary than in the Kapuas Kecil. Coarsening in both distributaries is a consequence of winnowing of fines (Figure 8). The grain size trend was not established for the Mendawat, because the surveyed section was insufficiently long. The skewness of the grain size distribution caused by the lack of grains larger 0.35 mm extends from the Kapuas Besar into the Kapuas Kecil and Kubu distributaries. However, while coarse material is completely absent in the Kubu distributary, the fraction of interspersed coarse material in the Kapuas Kecil is larger than in the Kapuas Besar. The Kubu distributary has no material larger than the mode of the distribution, contrary to the Kapuas Kecil case. This causes the downstream trends of standard deviation and skewness to be different in both distributaries, although they both coarsen, due to winnowing of fines (Figure 7). The standard deviation of the grain size distribution of the Kubu distributary is reduced, whereas it increases in the Kapuas Kecil. Similarly, the grain size distribution becomes more skewed toward coarser material in the Kubu distributary, while it becomes less skewed in the Kapuas Kecil. The grain size trends in the Kapuas Kecil breaks at 250 km, at the confluence with the Landak tributary.

## 4. Discussion

### 4.1. Comparison With the Mahakam Delta

*Rodríguez-Iturbe and Rinaldo* [2001] used an aerial photograph of the Kapuas alluvial plain to illustrate the complexity of delta channel networks. Following Galloway's classification [*Galloway*, 1975], the Kapuas delta is a mixed river tide-dominated delta, similar to the Mahakam Delta previously analyzed by *Sassi et al.* [2012]. Both these deltas on Borneo drain a similar catchment and are subject to similar forcing but show essential

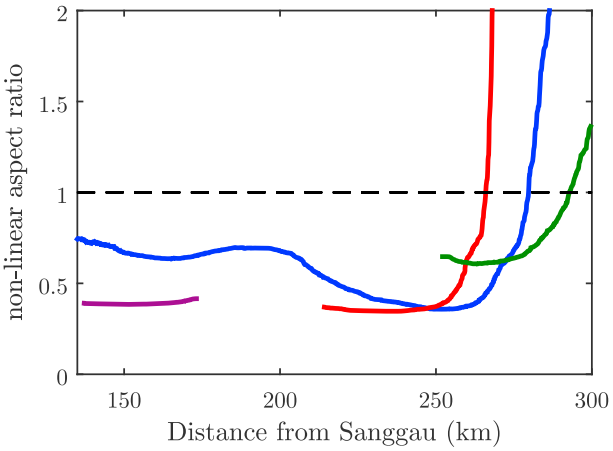


**Figure 10.** Nonlinear channel aspect ratio derived from empirical hydraulic geometry relationships. All distributaries are narrower and deeper in their upstream part then expected from the empirical relationship.

differences in their planforms. The Mahakam forms a single channel before branching into a large fan-shaped delta. The Kapuas River system has several distributaries branching off further upstream and only a small fan-shaped delta. In the Mahakam Delta, sinuous tidal channels can clearly be distinguished from nearly rectilinear fluvial distributaries (Figure 1). Such tidal creeks are absent in the Kapuas plain. The differences between the systems may relate to the geological constraints fixing the Mahakam River up until the delta apex, inhibiting avulsion and the formation of side distributaries [*Chambers et al.*, 2004]. Yet both rivers show an along-channel break of geometric scaling at a point where tidal influence becomes stronger than the river influence. Downstream of the break in the Kapuas, the increasing tidal influence is apparent from the gradual decrease of channel curvature toward the sea, which is similar to tidal meanders [*Marani et al.*, 2002]. The large trifurcation in the Kapuas delta-fan can be seen as an additional indication of a strong tidal influence in this reach [*Leonardi et al.*, 2013].

### 4.2. Comparison With Idealized Model Results

A comparison of the present topography of the Kapuas channel network with a historic map [*Hydrograaf*, 1907] shows that no substantial planform changes have occurred since 1882, suggesting that the river can be considered to be close to a dynamic morphodynamic equilibrium. This makes the Kapuas suitable for comparison with equilibrium river profiles. In the Kapuas, the width convergence breaks at the delta apex, which has implications for tidal propagation and sediment transport. The width reduction and depth increase are such that the cross-sectional area remains remarkably constant, especially in the Kapuas Besar. This is less so in the Kapuas Kecil, but the latter channel is subject to dredging. Idealized models of tidal channels often impose a fixed width that is continuously converging [*Seminara et al.*, 2012; *Bolla Pittaluga et al.*, 2014, 2015a]. For a model setup with a fixed width and constant discharge adopted by *Bolla Pittaluga et al.* [2014], equilibrium bed level profiles showed an adverse bed slope over a small section near the mouth bar region, which corresponds to a depth increase. Results from the Kapuas show the depth increase continues up to the point where width no longer converges, which is at a distance from the mouth that is small compared to the length over which the tide attenuates. The constancy of the cross-sectional area along the channels suggests that the aspect ratio is a key variable to be resolved in theoretical studies on equilibrium channel geometries.

### 4.3. Comparison With Hydraulic Geometry Relations

All Kapuas distributaries consist of a fluvial reach terminating in a tidal funnel. Comparison of the fluvial reaches to empirical hydraulic relationships allows to determine how similar the distributaries are to fluvial channels. Based on an elaborate review, *Eaton* [2013] introduced the following relations:

$$Q_{bf} = (w/3.35)^{(1/0.536)}$$
$$Q_{bf} = (h/0.305)^{(1/0.384)} \quad (1)$$

The ratio of discharges based on width and based on depth (respectively), $r$, then reads as

$$r = \frac{(w/3.35)^{(1/0.536)}}{(h/0.305)^{(1/0.384)}}. \quad (2)$$

The expected value of $r$ is 1 and does not depend on the channel size. $r > 1$ indicates an excess of width over depth, compared to alluvial channels without tides. Figure 10 shows the nonlinear width to depth ratio of the Kapuas distributaries. The width-to-depth ratio is larger in the upstream than in the downstream half of

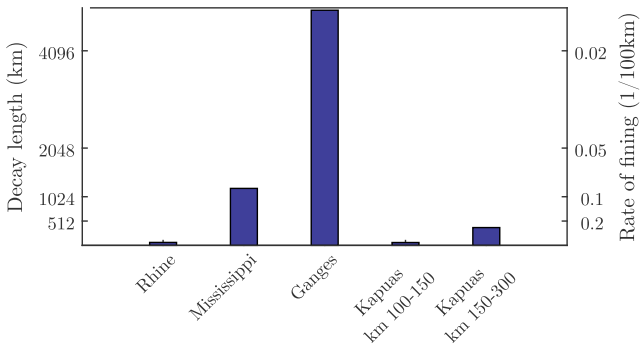


**Figure 11.** Comparison of downstream fining of bed material between the Kapuas and other large sand bed rivers (adopted from *Frings* [2008] and original data from *ten Brinke* [1997], *Nordin and Queen* [1992], and *Singh et al.* [2007]).

the alluvial plain. Upstream of the tidal funnels, the ratios of $r$ are smaller than one, which renders the river comparatively deep. The tides systematically adjust the aspect ratio far beyond the value characteristic for alluvial rivers, which can be seen as tidal channels having a depth excess.

### 4.4. Influence of Bifurcation Geometry on Sediment Division

The similarity of bed material in the branches of the distributaries indicates that the transport of bed material into the side distributaries is inhibited neither by the particular u shape of the bifurcations nor by the increase in bed level. Suspended load is typically the dominant mode of transport in meandering rivers, such as the Kapuas [*Schumm*, 1985]. The shape of the bifurcations is similar to the geometry of tie channel junctions connecting rivers to lakes [*Rowland and Dietrich*, 2005]. Unlike tie channels, the side distributaries of the Kapuas receive sufficient sediment to retain an active bed. The large-size and dense vegetation on the spits separating the side channel from the main river further indicate the long-term stability of the bifurcation and the role of cohesive banks in planform development. This particular topography is rare but can be observed in other rivers on Borneo and in the Niger Delta [*Abam*, 1999].

The bed material grain size is often discontinuous at river bifurcations, such as observed in the Rhine [*Frings and Kleinhans*, 2008]. At bifurcations with different bed level between the branches, the shallower branch receives fewer and finer material, as both the grain size and the concentration of suspended sediment decrease with vertical distance to the bed. The winnowing of fines in the Kubu and Kapuas Kecil confirms a low sediment supply to those channels. However, both in the Kapuas Kecil and in the Mendawat channel, the bed material is not finer than upstream of the respective bifurcation, only material in the Kubu branch is finer. Bend sorting can also contribute to differences of bed material in bifurcation branches. Branches located in outer bends receive fewer and coarser material [*Ikeda*, 1989; *Frings*, 2008]. The trend of bed material size in the main branch is not discontinuous across the Kapuas bifurcation. The limited influence of the bifurcations on the Kapuas Besar can be attributed to the small size of the side distributaries. The grain size in the Kapuas Kecil and the Mendawat channels, both branching off in outer bends, is only slightly larger than in the corresponding section of the main channel. The grain size in the Kubu at its inlet is even finer than in the corresponding section of the Kapuas Besar channel, although the Kapuas Besar is deeper and has coarser bed material at the inlet of Kubu. Thus, bend sorting may be less important in suspended load rivers. Other factors than bifurcation geometry, such as the phase difference of the tidal wave between the channels, may have an important influence on the division of sediment at bifurcations.

### 4.5. Sediment Transport Regime

The rapid decrease of the median grain size in the reach between km 110 and 150 is caused by selective deposition of material larger than 0.35 mm. Within this reach there is a strong reduction of the bankfull water surface slope (Figure 3a), as the river transits from the upstream valley to the alluvial plain (Figure 2). The reduction of grain size and widening of the river compensate for the reduction of the slope to maintain constant sediment transport. *Frings* [2008] gives the distance over which the grain size halves for several large sand bed rivers. Figure 11 compares the rate of fining and decay length to the base $e$. The rate of downstream fining in the alluvial plain of the Kapuas is large compared to other rivers. The alluvial plain of the Kapuas is shorter than of those of the rivers used for comparison, which may contribute to a more rapid reduction of the grain size. Downstream of 150 km, all remaining grain size fractions are transported and the rate of fining

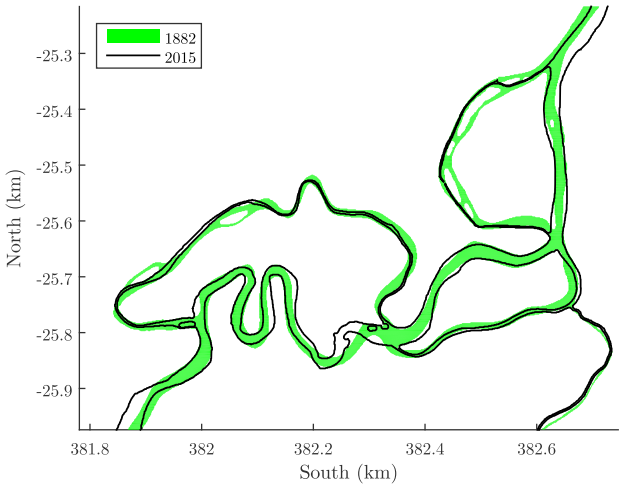


**Figure 12.** Three avulsion loops in the Kapuas located between 125 and 165 km downstream of Sanggau, in 1882 and 2015; in all loops one branch has been filled in, in strong contrast to distributaries connected to the sea, which do not have considerably changed their width over the same time span.

decreases. The continuation of downstream fining toward the river mouth suggests that tides have limited impact on the sediment sorting processes in the Kapuas distributaries, as strong tidal influence causes an increase of grain size toward the river mouth [*Dalrymple and Choi*, 2007].

### 4.6. Stability of the Distributary Channel Network

*Slingerland and Smith* [1998] developed a mathematical model for the initiation of river avulsion. They found that grain size influences the probability that following an avulsion both channels remain permanently open. In their model, avulsion was followed by quick abandonment of either of the two branches for grains of 0.1 mm, while for grain sizes of 0.4mm, both branches remained open, provided that the slope advantage of the new branch remains below a factor of 5. Median grain size in the Kapuas remains above 0.2 mm, suggesting that partial avulsions resulting in two stable branches are likely. Stable bifurcations obtain an asymmetric configuration, where one branch is larger than the other [*Wang et al.*, 1995; *Bolla Pittaluga et al.*, 2003; *Edmonds and Slingerland*, 2008; *Bolla Pittaluga et al.*, 2015b]. The Kapuas is no exception to this.

The increase of grain size due to winnowing of fines along the Kapuas Kecil and Kubu indicate that the sediment transport is directed seaward and that those channels are not aggrading. This corresponds to the observation that the side channels do not show any sign of infilling compared to the survey in 1882. This is in contrast to three small avulsion loops located in the upstream part of the alluvial plain that are not directly connected to the sea and have partially filled in since then (Figure 12). The morphological stability of channels in the Kapuas thus depends on whether channels reconnect before reaching the sea or not.

## 5. Conclusion

The Kapuas River forms a complex, natural channel network, consisting of one main stream and three side distributaries. Tides in the Kapuas strongly depend on discharge, ranging from nearly complete admittance during low flow to complete attenuation during high flow, toward the upstream end of the alluvial plain. This makes the Kapuas ideal to investigate channel geometry and bed material grain size in the fluvial-tidal transition zone. All distributaries of the Kapuas consist of a long and deep fluvial upstream reach and a short and shallow tidal funnel at the downstream end, which terminate in shallow mouth bars. In each distributary there is a clear break of channel geometrical properties between these two reaches, at which the channel width obtains a minimum and channel depth a maximum. Thus, the Kapuas distributaries are neither continuously converging, as in estuarine channels, nor nonconverging as in delta channels unaffected by tides. The Mahakam delta shows a similar break of channel geometry, indicating that this phenomenon may be a general characteristic of the fluvial-tidal transition. Trends of bed material grain size in the Kapuas were found not to be related to the channel geometry. Bed material in the main distributary shows a downstream fining trend, similar to that typically observed in rivers. There is no corresponding change of the grain size properties where the trend of downstream channel geometry breaks. Bed material in the side distributaries becomes coarser in the downstream direction, in contrast to the downstream fining in the main distributary. Differences in grain sizes between downstream branches may be caused by undersupply of sediment to the side distributaries, related to the asymmetric shape of bifurcations. Thus, in contrast to channel geometry, bed material grain size does strongly depend on the division of sediment at bifurcations.

**Acknowledgments**
This research was supported by the Royal Netherlands Academy of Arts and Sciences (KNAW) project SPIN3-JRP-29. The authors thank Hidayat for the processing of bed material samples at the Indonesian Institute of Sciences, as well as Muhammad Pramulya (Tanjungpura University), Laura Schlebes, and Judit Snethlage (both Wageningen University) for their field work support. We also thank Pieter Hazenberg (Wagening University) for technical support. We also thank the Editor, Giovanni Coco, and three anonymous reviewers for giving constructive feedback to the draft version of this manuscript. Preprocessed data, including a detailed description thereof, are provided as supporting information (SI) files. Bulk raw data are available from the first author (Wageningen University, Hydrology and Quantitative Water Management Group, P.O. box 47, 6700 AA Wageningen, The Netherlands, karl.kastner@wur.nl).

## References

Abam, T. K. S. (1999), Impact of dams on the hydrology of the Niger Delta, *Bull. Eng. Geol. Environ.*, *57*(3), 239–251.
Andren, H. (1994), Development of the Laitaure delta, Swedish Lappland: A study of growth, distributary forms and processes, PhD thesis, Uppsala Univ., Uppsala, Sweden.
Arce, G. R., Y.-T. Kim, and K. E. Barner (1998), Order-statistic filtering and smoothing of time-series: Part I, in *Order Statistics: Applications, Handbook of Statistics*, vol. *17*, pp. 525–554, Elsevier, Amsterdam, Netherlands, doi:10.1016/S0169-7161(98)17022-0.
American Society for Testing and Materials E11-16 (2016), *Standard Specification for Woven Wire Test Sieve Cloth and Test Sieves*, ASTM Int., West Conshohocken, Pa.
Bolla Pittaluga, M., R. Repetto, and M. Tubino (2003), Channel bifurcation in braided rivers: Equilibrium configurations and stability, *Water Resour. Res.*, *39*(3), 1046, doi:10.1029/2001WR001112.
Bolla Pittaluga, M., R. Luchi, and G. Seminara (2014), On the equilibrium profile of river beds, *J. Geophys. Res. Earth Surf.*, *119*, 317–332, doi:10.1002/2013JF002806.
Bolla Pittaluga, M., N. Tambroni, A. Canestrelli, R. Slingerland, S. Lanzoni, and G. Seminara (2015a), Where river and tide meet: The morphodynamic equilibrium of alluvial estuaries, *J. Geophys. Res. Earth Surf.*, *120*, 75–94, doi:10.1002/2014JF003233.
Bolla Pittaluga, M., G. Coco, and M. G. Kleinhans (2015b), A unified framework for stability of channel bifurcations in gravel and sand fluvial systems, *Geophys. Res. Lett.*, *42*, 7521–7536, doi:10.1002/2015GL065175.
Buschman, F. A., A. J. F. Hoitink, S. M. de Jong, P. Hoekstra, H. Hidayat, and M. G. Sassi (2012), Suspended sediment load in the tidal zone of an Indonesian river, *Hydrol. Earth Syst. Sci.*, *16*(11), 4191–4204.
Chambers, J. L. C., I. Carter, I. R. Cloke, J. Craig, S. J. Moss, and D. W. Paterson (2004), Thin-skinned and thick-skinned inversion-related thrusting—A structural model for the Kutai Basin, Kalimantan, Indonesia, *Thrust Tectonics and Hydrocarbon Systems: AAPG Mem.*, *82*, 614–634.
Coleman, J. M. (1988), Dynamic changes and processes in the Mississippi River delta, *Geol. Soc. Am. Bull.*, *100*(7), 999–1015.
Costard, F., and E. Gautier (2007), The Lena River: Hydromorphodynamic features in a deep permafrost zone, in *Large Rivers: Geomorphology and Management*, edited by A. Gupta, pp. 225–233, John Wiley Ltd., Sussex, England, doi:10.1002/9780470723722.ch11.
D'Alpaos, A., S. Lanzoni, M. Marani, S. Fagherazzi, and A. Rinaldo (2005), Tidal network ontogeny: Channel initiation and early development, *J. Geophys. Res.*, *110*, F02001, doi:10.1029/2004JF000182.
D'Alpaos, A., S. Lanzoni, M. Marani, and A. Rinaldo (2009), On the O'Brien–Jarrett–Marchi law, *Rend. Lincei*, *20*(3), 225–236.
Dalrymple, R. W., and K. Choi (2007), Morphologic and facies trends through the fluvial–marine transition in tide-dominated depositional systems: A schematic framework for environmental and sequence-stratigraphic interpretation, *Earth Sci. Rev.*, *81*(3), 135–174.
Dalrymple, R. W., D. A. Mackay, A. A. Ichaso, and K. S. Choi (2012), Processes, morphodynamics, and facies of tide-dominated estuaries, in *Principles of Tidal Sedimentology*, pp. 79–107, Springer, Dordrecht, Netherlands.
Davies, G., and C. D. Woodroffe (2010), Tidal estuary width convergence: Theory and form in north Australian estuaries, *Earth Surf. Proc. Land.*, *35*(7), 737–749.
Davis Jr., R. A., and R. W. Dalrymple (Eds.) (2011), *Principles of Tidal Sedimentology*.
Eaton, B. C. (2013), Hydraulic geometry: Empirical investigations and theoretical approaches, in *Treatise on Geomorphology*, vol. 9, edited by J. F. Shroder and E. Wohl, pp. 313–329, Academic Press, San Diego, Calif, doi:10.1016/B978-0-12-374739-6.00235-9.
Edmonds, D. A., and R. L. Slingerland (2007), Mechanics of river mouth bar formation: Implications for the morphodynamics of delta distributary networks, *J. Geophys. Res.*, *112*, F02034, doi:10.1029/2006JF000574.
Edmonds, D. A., and R. L. Slingerland (2008), Stability of delta distributary networks and their bifurcations, *Water Resour. Res.*, *44*, W09426, doi:10.1029/2008WR006992.
Egbert, G. D., and S. Y. Erofeeva (2002), Efficient inverse modeling of barotropic ocean tides, *J. Atmos. Oceanic Technol.*, *19*(2), 183–204.
Emmerton, C. A., L. F. W. Lesack, and P. Marsh (2007), Lake abundance, potential water storage, and habitat distribution in the Mackenzie River delta, western Canadian Arctic, *Water Resour. Res.*, *43*, W05419, doi:10.1029/2006WR005139.
Fagherazzi, S. (2008), Self-organization of tidal deltas, *Proc. Natl. Acad. Sci. U.S.A.*, *105*(48), 18,692–18,695.
Fagherazzi, S., and D. J. Furbish (2001), On the shape and widening of salt marsh creeks, *J. Geophys. Res.*, *106*(C1), 991–1003.
Frings, R. M. (2008), Downstream fining in large sand-bed rivers, *Earth Sci. Rev.*, *87*(1), 39–60.
Frings, R. M., and M. G. Kleinhans (2008), Complex variations in sediment transport at three large river bifurcations during discharge waves in the river Rhine, *Sedimentology*, *55*(5), 1145–1171.
Galloway, W. E. (1975), Process framework for describing the morphologic and stratigraphic evolution of deltaic depositional systems, in *Deltas: Models for Exploration*, pp. 87–98, Houston Geol. Soc., Houston, Tex.
Geleynse, N., J. E. A. Storms, D.-J. R. Walstra, H. R. A. Jagers, Z. B. Wang, and M. J. F. Stive (2011), Controls on river delta formation: Insights from numerical modelling, *Earth Planet. Sci. Lett.*, *302*(1), 217–226.
Hack, J. T. (1957), Studies of longitudinal stream profiles in Virginia and Maryland, *Tech. Rep. 294-B*, U.S. Government Printing Office, Washington.
Hidayat, H. H., et al. (2016), Hydrology of inland tropical lowlands: The Kapuas and Mahakam wetlands, *Hydrol. Earth Syst. Sci. Discuss.*, *21*, 765–777, doi:10.5194/hess-2016-388.
Hoitink, A. J. F., and D. A. Jay (2016), Tidal river dynamics: Implications for deltas, *Rev. Geophys.*, *54*, 240–272, doi:10.1002/2015RG000507.
Hydrograaf (1907), *Westkust Borneo*, Blad III, Pontianak tot Eiland Maya, 1882.
Ikeda, S. (1989), Sediment transport and sorting at bends, in *River Meandering*, pp. 103–125, AGU, Washington, D. C., doi:10.1029/WM012p0103.
Jarrett, J. T. (1976), Tidal prism-inlet area relationships, *Tech. Rep.*, DTIC Document.
Kukulka, T., and D. A. Jay (2003a), Impacts of Columbia River discharge on salmonid habitat: 1. A nonstationary fluvial tide model, *J. Geophys. Res.*, *108*(C9), 3293, doi:10.1029/2002JC001382.
Kukulka, T., and D. A. Jay (2003b), Impacts of Columbia River discharge on salmonid habitat: 2. Changes in shallow-water habitat, *J. Geophys. Res.*, *108*(C9), 3294, doi:10.1029/2003JC001829.
Leonardi, N., A. Canestrelli, T. Sun, and S. Fagherazzi (2013), Effect of tides on mouth bar morphology and hydrodynamics, *J. Geophys. Res. Oceans*, *118*(9), 4169–4183, doi:10.1002/jgrc.20302.
Leopold, L. B., and T. Maddock Jr. (1953), *The Hydraulic Geometry of Stream Channels and Some Physiographic Implications, Prof. Pap. 252*, U.S. Govt. Print. Off., Washington, D. C.
Makaske, B. (2001), Anastomosing rivers: A review of their classification, origin and sedimentary products, *Earth Sci. Rev.*, *53*(3), 149–196.
Marani, M., S. Lanzoni, D. Zandolin, G. Seminara, and A. Rinaldo (2002), Tidal meanders, *Water Resour. Res.*, *38*(11), 1225, doi:10.1029/2001WR000404.

Marciano, R., Z. B. Wang, A. Hibma, H. J. de Vriend, and A. Defina (2005), Modeling of channel patterns in short tidal basins, *J. Geophys. Res.*, *110*, F01001, doi:10.1029/2003JF000092.
McLaren, P. (1981), An interpretation of trends in grain size measures, *J. Sediment. Res.*, *51*(2), 611–624.
Mikhailov, V. N. (1966), Hydrology and formation of river mouth bars, *Problems Humid Trop. Zone Deltas*, *1*, 59–64.
Mikhailov, V. N. (1970), Hydrologic-morphometric characteristics of delta branches, *Stud. Rep. Hydrol.*, *9*, 146–158.
Myrick, R. M., and L. B. Leopold (1963), Hydraulic geometry of a small tidal estuary, *Tech. Rep.*, U.S. Govt. Print. Off.
Nordin, C. F., and B. S. Queen (1992), Particle size distributions of bed sediments along the thalweg of the Mississippi River, Cairo, Illinois, to head of passes, September 1989, *Tech. Rep.*, DTIC Document.
Olariu, C., and J. P. Bhattacharya (2006), Terminal distributary channels and delta front architecture of river-dominated delta systems, *J. Sediment. Res.*, *76*(2), 212–233.
Orton, G. J., and H. G. Reading (1993), Variability of deltaic processes in terms of sediment supply, with particular emphasis on grain size, *Sedimentology*, *40*(3), 475–512.
Passalacqua, P., S. Lanzoni, C. Paola, and A. Rinaldo (2013), Geomorphic signatures of deltaic processes and vegetation: The Ganges-Brahmaputra-Jamuna case study, *J. Geophys. Res. Earth Surf.*, *118*, 1838–1849.
Pillsbury, G. B. (1940), *Tidal Hydraulics*, vol. 34, U.S. Govt. Print. Off., Wash.
Pugh, D. T. (1987), *Tides, Surges and Mean Sea-Level: A Handbook for Engineers and Scientists*, John Wiley, Chichester, U. K.
Roberts, H. H., R. D. Adams, and R. H. W. Cunningham (1980), Evolution of sand-dominant subaerial phase, Atchafalaya Delta, Louisiana, *AAPG Bull.*, *64*(2), 264–279.
Rodríguez-Iturbe, I., and A. Rinaldo (2001), *Fractal River Basins: Chance and Self-Organization*, Cambridge Univ. Press, Cambridge.
Rowland, J. C., and W. E. Dietrich (2005), The evolution of a tie channel, *River Coastal Estuarine Morphodyn. RCEM*, *1*, 725–736.
Sassi, M. G., A. J. F. Hoitink, B. Brye, and E. Deleersnijder (2012), Downstream hydraulic geometry of a tidally influenced river delta, *J. Geophys. Res.*, *117*, F04022, doi:10.1029/2012JF002448.
Savenije, H. H. G., M. Toffolon, J. Haas, and E. J. M. Veling (2008), Analytical description of tidal dynamics in convergent estuaries, *J. Geophys. Res.*, *113*, C10025, doi:10.1029/2007JC004408.
Schumm, S. A. (1985), Patterns of alluvial rivers, *Annu. Rev. Earth Planet. Sci.*, *13*, 5–27.
Scott, D. W. (2015), *Multivariate Density Estimation: Theory, Practice, and Visualization*, John Wiley, New York.
Seminara, G., M. B. Pittaluga, and N. Tambroni (2012), Morphodynamic equilibrium of tidal channels, in *Environmental Fluid Meechanics-Memorial Volume in Honour of Prof. Gerhard Jirka*, edited by W. Rodi and M. Uhlmann, pp. 153–174, CRC Press, Karslruhe, Germany.
Shaw, J. B., D. Mohrig, and R. W. Wagner (2016), Flow patterns and morphology of a prograding river delta, *J. Geophys. Res. Earth Surf.*, *121*(2), 372–391, doi:10.1002/2015JF003570.
Singh, M., I. B. Singh, and G. Müller (2007), Sediment characteristics and transportation dynamics of the Ganga River, *Geomorphology*, *86*(1), 144–175.
Slingerland, R., and N. D. Smith (1998), Necessary conditions for a meandering-river avulsion, *Geology*, *26*(5), 435–438.
Snow, R. S., and R. L. Slingerland (1987), Mathematical modeling of graded river profiles, *J. Geol.*, *1995*(1), 15–33.
Stevaux, J. C., and I. A. Souza (2004), Floodplain construction in an anastomosed river, *Quatern. Int.*, *114*(1), 55–65.
Stouthamer, E., K. M. Cohen, and M. J. P. Gouw (2011), Avulsion and its implications for fluvial-deltaic architecture: Insights from the Holocene Rhine-Meuse delta, *SEPM Spec. Publ.*, *97*, 215–232.
ten Brinke, W. B. M. (1997), *De bodemsamenstelling van Waal en IJssel in de jaren 1966, 1976, 1984 en 1995*, 158 pp., RIZA Arnhem, Nederlands.
Vermeulen, B., A. J. F. Hoitink, S. W. Berkum, and H. Hidayat (2014), Sharp bends associated with deep scours in a tropical river: The river Mahakam (East Kalimantan, Indonesia), *J. Geophys. Res. Earth Surf.*, *119*, 1441–1454, doi:10.1002/2013JF002923.
Wang, S., J. Ni, G. Wang, D. Cheng, and O. Zhang (2004), Hydrological processes of an anastomosing river system on the Zhujiang River delta, China, *J. Coastal. Res.*, *Special issue 43: Tidal Dynamics and Environment*, 124–133.
Wang, Z. B., M. De Vries, R. J. Fokkink, and A. Langerak (1995), Stability of river bifurcations in 1D morphodynamic models, *J. Hydraul. Res.*, *33*(6), 739–750, doi:10.1080/00221689509498549.
Wilkerson, G. V., and G. Parker (2010), Physical basis for quasi-universal relationships describing bankfull hydraulic geometry of sand-bed rivers, *J. Hydraul. Eng.*, *137*(7), 739–753.
Wright, L. D., J. M. Coleman, and B. G. Thom (1973), Processes of channel development in a high-tide-range environment: Cambridge Gulf-Ord River Delta, Western Australia, *J. Geol.*, *81*(1), 15–41.
Xiaoqing, Y., and X. Yang (2003), Manual on sediment management and measurement, 158 pp., Secretariat of the World Meteorological Organization, Univ. of Calif.